

See discussions, stats, and author profiles for this publication at: <https://www.researchgate.net/publication/23081184>

# Use of a Symmetry Condition to Compute the Conformation of Gramicidin S

ARTICLE *in* MACROMOLECULES · NOVEMBER 1975

Impact Factor: 5.8 · DOI: 10.1021/ma60048a016 · Source: PubMed

---

CITATIONS

119

---

READS

7

3 AUTHORS, INCLUDING:



Nobuhiro Go

Japan Atomic Energy Agency

238 PUBLICATIONS 9,934 CITATIONS

SEE PROFILE

which gave a similar spectrum) shows only a single  $\alpha$  CH peak despite two of equal intensity being observed in  $\text{CDCl}_3$ . It follows that both the "correct" and "wrong" sense residues have the same or a similar chemical shift. The slightly racemized alternating DL-7 shows two  $\alpha$  CH peaks of unequal intensity (very much as in  $\text{CDCl}_3$ ) equal to high field and low field of the single maximum of  $\text{LD}_{\text{cat}}$  II. By analogy with the spectra in  $\text{CDCl}_3$  it is concluded that the  $\alpha$  CH of  $\text{LD}_{\text{cat}}$  II is an unresolved symmetrical doublet, the components of which are at the shifts shown by DL-7 (3.95 and 3.79 ppm) and can be assigned to residues on their "correct" and "wrong"  $\alpha$  helical sense. The spectrum of LDL in  $\text{DMF-d}_7$  also shows a strong resemblance to that in  $\text{CDCl}_3$ : there are two NH peaks of very different shift which have an intensity ratio of 2:1 and the  $\alpha$  CH spectrum shows a peak (4.03 ppm) not observed in  $\text{LD}_{\text{cat}}$  II or DL-7 that has a shift close to that found for PBLG. The general conclusion to be drawn is therefore that the conformations taken up by the polymers in  $\text{DMF-d}_7$  do not differ greatly from those in  $\text{CDCl}_3$ , i.e., all the polymers are  $\alpha$  helical. Furthermore, there is no sign at 57°C of a low-field  $\alpha$  CH resonance that would indicate a transconformational change to the  $\pi_{\text{DL}}$  helix.

### Conclusion

It has been previously demonstrated that benzyl D,L-glutamates both random and alternating are largely helical in chloroform solution and it was proposed that they form a distorted helix. By the use of alternating copolymers having an almost negligible degree of racemization ( $\text{LD}_{\text{cat}}$ ) it has been possible to interpret the complex  $\alpha$  CH spectrum obtained in chloroform/0.5% TFA and thereby establish the  $\alpha$  CH spectral features characteristic of the  $\alpha$  helix built with D and L residues: a spectrum with two peaks assignable to residues on the "correct (3.82 ppm)" and "wrong (3.65 ppm)" helix sense. These two peaks cannot be assigned to the coexistence of helix and coil as demonstrated by the addition of TFA to promote the helix-coil transition. Since the  $\text{LD}_{\text{cat}}$  copolymers show no  $\alpha$  CH resonance characteristic of the normal PBLG helix (3.95 ppm), it is concluded that in  $\text{CDCl}_3$ /0.5% TFA they are entirely in the form of the characteristic  $\alpha$  helix of poly(D-L-peptides).

The presence of some racemization in an alternating copolymer (DL-7) leads to a greater proportion of residues being on the "correct" sense  $\alpha$  helix and to the occurrence of some regular  $\alpha$  helix as seen from the presence of a weak overlapped component at about 3.9 ppm. In the case of random D,L copolymers, the proportion of the poly(D-L-peptide)  $\alpha$  helix is much less as seen for example from the low intensity of the 3.65 ppm component in the LD 80/20 copolymer.

The spectra of the  $\text{LD}_{\text{cat}}$  polymers in dioxane (Figure 4) reveal the presence of the  $\pi_{\text{DL}}$  helix by a new peak at 4.45 ppm (a very low shift for helix) and demonstrate that the temperature induced  $\alpha \rightarrow \pi_{\text{DL}}$  transition of  $\text{LD}_{\text{cat}}$  II is not complete at 86°C. The spectra in dimethylformamide show strong similarities to those in chloroform and it is concluded that the conformations in the two solvents are similar. In particular there is no evidence in either solvent for the presence of the  $\pi_{\text{DL}}$  helix.

**Acknowledgment.** We are grateful to Drs. E. M. Bradbury and G. Spach for helpful discussions and continuous interest in this work. P.D.C. and C.C.R. acknowledge the support of the Science Research Council of Great Britain.

### References and Notes

- (1) (a) Centre de Biophysique Moléculaire; (b) Portsmouth Polytechnic.
- (2) (a) F. A. Bovey, J. J. Ryan, G. Spach, and F. Heitz, *Macromolecules*, **4**, 433 (1971); (b) L. Paolillo, P. Temussi, E. Trivellone, E. M. Bradbury, and C. Crane-Robinson, *Macromolecules*, **6**, 831 (1973).
- (3) P. M. Hardy, J. C. Haylock, D. I. Marlborough, H. N. Rydon, H. T. Storey, and R. C. Thompson, *Macromolecules*, **4**, 435 (1971).
- (4) A. Caille, F. Heitz, and G. Spach, *J. Chem. Soc., Perkin Trans. 1*, 1621 (1974).
- (5) Y. Trudelle, *J. Chem. Soc., Perkin Trans. 1*, 1001 (1973).
- (6) F. Heitz and G. Spach, *preceding paper in this issue* (1975).
- (7) G. Spach, *C. R. Hebd. Séances Acad. Sci.*, **249**, 543 (1959).
- (8) H. Benoit, L. Freund, and G. Spach, "Poly- $\alpha$ -amino Acids", G. D. Fasman Ed., Marcel Dekker, New York, N.Y., 1971, p 105.
- (9) F. Heitz and G. Spach, *Macromolecules*, **4**, 429 (1971).
- (10) F. Heitz, Thesis, Orléans, 1974.
- (11) A. R. Downie, A. Elliott, W. E. Hanby, and B. R. Malcolm, *Proc. R. Soc. London, Ser. A*, **242**, 325 (1957).
- (12) F. Heitz, B. Lotz, and G. Spach, *J. Mol. Biol.*, **92**, 1 (1975).
- (13) L. Paolillo, P. Temussi, E. Trivellone, E. M. Bradbury, and C. Crane-Robinson, *Biopolymers*, **10**, 2555 (1971).
- (14) E. M. Bradbury, B. G. Carpenter, C. Crane-Robinson, and H. Goldman, *Macromolecules*, **4**, 557 (1971).
- (15) E. M. Bradbury, C. Crane-Robinson, and P. G. Hartman, *Polymer*, **14**, 543 (1973).

## Use of a Symmetry Condition to Compute the Conformation of Gramicidin S<sup>1</sup>

Mary Dygert,<sup>2</sup> Nobuhiro Gō, and Harold A. Scheraga\*

Department of Chemistry, Cornell University, Ithaca, New York 14853. Received May 6, 1975

**ABSTRACT:** Using an improved method for computing conformations of closed rings with symmetry, in conjunction with an improved empirical energy function, the conformational space of Gramicidin S is reexamined. The search for minimum energy conformations is confined to the subspace containing closed symmetric rings. A large number of initial conformations selected from that subspace is subjected to energy minimization or is eliminated in a sequence of steps designed to locate the global minimum-energy conformation. One conformation having distinctly low energy is found and is judged to be the global minimum-energy conformation. This conformation is of the  $\beta$ -pleated sheet type and is in complete agreement with experimental data. Similar structures with  $\beta$ -pleated sheet-type conformations have been proposed previously on the basis of less extensive examinations of the conformational space; the condition of exact ring closure, and the extensive examination of conformational space, used here, establish this structure on a firm basis.

The conformation of Gramicidin S (Gr-S), a cyclosymmetric decapeptide antibiotic, has been studied extensively in recent years both experimentally and by conformational

energy calculations. The cyclosymmetric nature of Gr-S makes it an ideal system for conformational energy calculations since the cyclic structure imposes constraints on the

accessible conformational space, while the property of symmetry reduces the number of variables and pairwise atomic interactions considerably. Although a variety of techniques have been employed to generate molecules possessing closed rings of proper symmetry, none of these has provided mathematically exact ring closure. Recently, we have developed a mathematical technique for finding sets of dihedral angles which will generate a molecule possessing both exact ring closure and proper symmetry.<sup>3</sup> By computing the dihedral angles necessary for ring closure with symmetry, the need for an artificial ring-closing potential is eliminated. Furthermore, since the dihedral angles required for closure are dependent variables, the total number of independent variables to be considered is reduced. These improvements enable the conformational space to be examined more thoroughly since the search is confined to those regions in which the symmetry equations have solutions.

Previous theoretical investigations of this molecule have relied initially on the chance closure of rings. Actual closure was obtained by applying a ring-closing potential, or by minimizing the end-to-end distance, in conformations that were found to have nearly closed rings. Thus, many conformations were not considered because they failed to satisfy the initial requirement of a nearly closed ring. By obtaining mathematically closed rings at the outset, this element of chance is eliminated from the computations reported here. In addition to the development of mathematically rigorous ring closure techniques, we have developed an improved set of energy parameters for nonbonded, hydrogen-bond, electrostatic, and torsional potentials in polypeptides and proteins.<sup>4,5</sup> The purpose of this paper is to report the results of a systematic search for minimum energy conformations of Gr-S using these improved methods.

## I. Methods

**A. Outline of the Methods.** A schematic representation of Gr-S is shown in Figure 1. The sequence is comprised of a pentapeptide chain repeated twice to form the cyclic decapeptide  $(\text{-Val-Orn-Leu-D-Phe-Pro-})_2$ . Although the symmetric sequence does not necessarily imply a symmetric conformation, X-ray crystallographic<sup>6</sup> studies indicate the existence of a two-fold axis of symmetry in the crystalline state. The absence of any doubling of resonances for pairs of like residues both in  $^1\text{H}$  NMR<sup>7,8</sup> and  $^{13}\text{C}$  NMR<sup>9</sup> spectra demonstrates that the  $C_2$  symmetry is also present in solution.

Two assumptions are made prior to generation of symmetric backbone conformations. First, the conformation at all secondary amide groups is taken fixed as trans. For the residues Val, Orn, Leu, and D-Phe this is not an unreasonable assumption for energetic reasons; however, for the X-Pro peptide bond, the cis and trans isomers are both energetically possible. The chemical shifts of the  $\beta$  and  $\gamma$  carbons of proline in  $^{13}\text{C}$  NMR spectra demonstrate unequivocally that only one isomer is present and that it is most likely the trans form.<sup>10</sup> Second, the geometry [bond lengths, bond angles, and planar trans ( $\omega = 180^\circ$ ) peptide group] is maintained fixed, and corresponds to that reported by Momany et al.<sup>4</sup> based on a study of crystal structures of many model compounds. The convention used throughout this paper is that adopted by an IUPAC-IUB Commission.<sup>11</sup>

The search for minimum-energy conformations is carried out in four discrete steps. In the first two steps, instead of treating cyclodecapeptide  $(\text{-Val-Orn-Leu-D-Phe-Pro-})_2$ , we study a backbone molecule  $(\text{-Ala-Ala-Ala-D-Ala-Pro-})_2$  obtained by replacing the side chains of non-prolyl residues

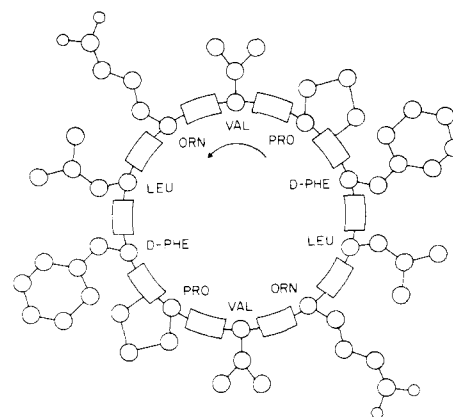


**Figure 1.** Sequence of Gramicidin S.  $\circ$  represents  $\text{CH}$ ,  $\text{CH}_2$ , or  $\text{CH}_3$  groups.  $\square$  represents the peptide  $\text{-CONH-}$  or  $\text{-CON-}$  group. The arrow indicates the usual direction of the sequence from the N to C terminus.

by methyl groups. In the process of this replacement, the values of the bond angles  $\tau[\text{NC}^\alpha\text{C}']$  for each type of residue (as given in ref 4) are kept unchanged (i.e., are not adjusted to that of alanine even though the side chain is that of alanine). The confinement of our attention to the backbone molecule in the first two steps of the search for minimum-energy conformations is assumed to be justifiable by the plausible argument that the backbone contribution dominates the total conformational energy. In the first step, many starting conformations of the backbone molecules are generated by solving the symmetry equations for a large number of sets of independent variables, which are selected by three different strategies; this step is described in section I-E. In the second step, these conformations are subjected to classification, grouping, and energy minimization. In this step all hydrogen atoms covalently bound to aliphatic and aromatic carbons are absorbed into the carbon atoms, and appropriate energy parameters corresponding to the united-atom treatment are used; this step is described in sections I-F and I-G. In the third step, side chains are generated onto the energetically stable backbones, and energy minimization is continued while still using the united atom approximation; this step is described in section I-H. Finally, in the fourth step, the minimum energy conformations obtained in the third step are refined by removing the united-atom approximation and minimizing the conformational energy with all atoms treated individually; this fourth step is described in section I-I.

**B. Generation of Symmetrical Backbone Conformations.** If the side chains of this molecule are temporarily disregarded, if  $\phi$  is taken as fixed at  $-75^\circ$  for the "down" puckering of the pyrrolidine ring of Pro,<sup>4</sup> and if all the peptide bonds are maintained in the planar trans conformation, then there are 18 backbone dihedral angles about which rotation can occur. The backbone contains three kinds of units in the sense described in ref 3, viz.,  $\text{CHR}_j$ ,  $\text{CONH}$ , and  $\text{CO-Pro}$ , where  $R_j$  represents the particular amino acid side chain and Pro refers to the pyrrolidine ring of proline. These units are linked by single bonds about which rotation can occur. The dihedral angle for rotation about the  $i$ th bond is denoted by  $\omega_i$  in this section. This meaning of  $\omega_i$  in this section is not to be confused with its usage, as the dihedral angle for rotation about a peptide bond, in the IUPAC-IUB nomenclature.<sup>11</sup> If these three types of units are designated by the symbols  $F_1$ ,  $F_2$ , and  $F_3$ , respectively, then Gr-S may be represented schematically by

$$(\text{F}_1/\text{F}_2\text{F}_1/\text{F}_2\text{F}_1/\text{F}_2\text{F}_1/\text{F}_3\text{F}_2)_2 \quad (1)$$

where the superscript  $j$  distinguishes the individual amino acid side chains from one another. There is associated with each of these 18 units a local coordinate system as defined in ref 3. The cartesian coordinates of each atom in the local coordinate systems correspond to those reported by Momany et al.<sup>4</sup> Having thus defined each local coordinate system, the appropriate transformation matrices providing relationships between a position vector  $\mathbf{r}_i$  in the  $i$ th coordinate system and the corresponding vector  $\mathbf{r}_{i-1}$  in the adjacent system can be determined easily. Here there are three types of such relationships depending upon whether the expression relates local coordinate systems of the type  $F_2$  to  $F_1^j$ ,  $F_1^j$  to  $F_2$ , or  $F_2$  to  $F_3$ . (The transformation  $F_3$  to  $F_1^j$  is identical with  $F_2$  to  $F_1^j$ .) These three relationships have the general form

$$\mathbf{r}_{i-1} = \mathbf{T}_{i-1} \mathbf{R}_i \mathbf{r}_i + \mathbf{p}_{i-1} \quad (2)$$

where  $\mathbf{T}_{i-1}$  is a  $3 \times 3$  orthogonal matrix (whose elements depend only on bond angles) that is used to rotate the  $i$ th coordinate system into the same orientation as that of the  $(i-1)$ th coordinate system after the intervening dihedral angle  $\omega_i$  has been rotated to zero.  $\mathbf{R}_i$ , the matrix to vary that intervening dihedral angle ( $\omega_i$ ) to zero, is given by

$$\mathbf{R}_i \equiv \mathbf{R}(\omega_i) = \begin{bmatrix} 1 & 0 & 0 \\ 0 & \cos \omega_i & -\sin \omega_i \\ 0 & \sin \omega_i & \cos \omega_i \end{bmatrix} \quad (3)$$

The vector  $\mathbf{p}_{i-1}$  is the position vector of the origin of the  $i$ th coordinate system with respect to the  $(i-1)$ th coordinate system. By repetitive use of equations of this form, a product matrix  $\mathbf{U}$  and vector  $\mathbf{p}$  can be generated to express the relationship between the symmetrically related 0th and  $m$ th coordinate systems

$$\mathbf{r}_0 = \mathbf{U} \mathbf{r}_m + \mathbf{p} \quad (4)$$

where

$$\mathbf{U} = \mathbf{T}_0 \mathbf{R}_1 \mathbf{T}_1 \mathbf{R}_2 \mathbf{T}_2 \mathbf{R}_3 \dots \mathbf{T}_{m-1} \mathbf{R}_m \quad (5)$$

and

$$\mathbf{p} = \mathbf{p}_0 + \mathbf{T}_0 \mathbf{R}_1 \mathbf{p}_1 + \mathbf{T}_0 \mathbf{R}_1 \mathbf{T}_1 \mathbf{R}_2 \mathbf{p}_2 + \dots + \mathbf{T}_0 \mathbf{R}_1 \mathbf{T}_1 \mathbf{R}_2 \mathbf{T}_2 \mathbf{R}_3 \mathbf{p}_3 \dots \mathbf{T}_{m-2} \mathbf{R}_{m-1} \mathbf{p}_{m-1} \quad (6)$$

The matrix  $\mathbf{U}$  brings the  $m$ th coordinate system into the same orientation as that of the 0th one, and the vector  $\mathbf{p}$  is the position vector of the origin of the  $m$ th coordinate system with respect to the 0th one. For Gr-S, since  $\phi$  of Pro and all  $\omega$ 's of peptide bonds are held fixed, the number of dihedral angles in a symmetry unit is 9 (i.e.,  $m = 9$ ). Therefore, the 0th and the 9th local coordinate systems must be made to overlap by a rotation of  $180^\circ$  about the  $C_2$  symmetry axis. In order to achieve this overlap,  $\mathbf{U}$  and  $\mathbf{p}$  must satisfy specific conditions, which can be regarded as conditions that the dihedral angles must satisfy, since  $\mathbf{U}$  and  $\mathbf{p}$  are generated from these dihedral angles by eq 2-6. The derivation of the necessary and sufficient conditions that  $\mathbf{U}$  and  $\mathbf{p}$  must satisfy in order to generate a cyclic structure with  $C_n$  symmetry is given in ref 3. It is shown there that, for the case of  $C_2$  symmetry, those conditions reduce to the single vector equation

$$(\mathbf{I} + \mathbf{U}) \mathbf{p} = 0 \quad (7)$$

where  $\mathbf{I}$  is the identity matrix. This equation can be solved analytically (see Appendix I) to give explicit formulas for the two dependent variables in terms of the independent ones (seven in this case). In ref 3, an example is given in which the dependent variables  $\omega_{m-1}$  and  $\omega_m$  are found in

terms of the independent variables  $\omega_1, \dots, \omega_{m-2}$ . Using the same notation as given in that paper, we shall solve for  $\omega_3$  and  $\omega_9$  in terms of  $\omega_1, \omega_2, \omega_4, \dots, \omega_8$  in order to illustrate that the unknowns need not be adjacent variables along the chain. In this special case, we shall denote  $\mathbf{R}_3$  as  $\mathbf{X}$  and  $\mathbf{R}_9$  as  $\mathbf{Y}$ . Then  $\mathbf{U}$  and  $\mathbf{p}$  of eq 5 and 6 can be expressed as

$$\mathbf{U} = \mathbf{A} \mathbf{X} \mathbf{B} \mathbf{Y} \quad (8)$$

$$\mathbf{p} = \mathbf{a} + \mathbf{A} \mathbf{X} \mathbf{b} \quad (9)$$

where

$$\mathbf{A} = \mathbf{T}_0 \mathbf{R}_1 \mathbf{T}_1 \mathbf{R}_2 \mathbf{T}_2 \quad (10)$$

$$\mathbf{B} = \mathbf{T}_3 \mathbf{R}_4 \mathbf{T}_4 \mathbf{R}_5 \mathbf{T}_5 \mathbf{R}_6 \mathbf{T}_6 \mathbf{R}_7 \mathbf{T}_7 \mathbf{R}_8 \mathbf{T}_8 \quad (11)$$

$$\mathbf{a} = \mathbf{p}_0 + \mathbf{T}_0 \mathbf{R}_1 \mathbf{p}_1 + \mathbf{T}_0 \mathbf{R}_1 \mathbf{T}_1 \mathbf{R}_2 \mathbf{p}_2 \quad (12)$$

$$\mathbf{b} = \mathbf{p}_3 + \mathbf{T}_3 \mathbf{R}_4 \mathbf{p}_4 + \mathbf{T}_3 \mathbf{R}_4 \mathbf{T}_4 \mathbf{R}_5 \mathbf{p}_5 + \mathbf{T}_3 \mathbf{R}_4 \mathbf{T}_4 \mathbf{R}_5 \mathbf{T}_5 \mathbf{R}_6 \mathbf{p}_6 + \mathbf{T}_3 \mathbf{R}_4 \mathbf{T}_4 \mathbf{R}_5 \mathbf{T}_5 \mathbf{R}_6 \mathbf{T}_6 \mathbf{R}_7 \mathbf{p}_7 + \mathbf{T}_3 \mathbf{R}_4 \mathbf{T}_4 \mathbf{R}_5 \mathbf{T}_5 \mathbf{R}_6 \mathbf{T}_6 \mathbf{R}_7 \mathbf{T}_7 \mathbf{R}_8 \mathbf{p}_8 \quad (13)$$

The problem then is to solve for the unknown quantities ( $\omega_3$  and  $\omega_9$ , in this example) in terms of the given quantities  $\mathbf{A}$ ,  $\mathbf{B}$ ,  $\mathbf{a}$ , and  $\mathbf{b}$ . The solution(s) is found by the equations given in Appendix I which, when satisfied, result in either one or two solutions. The subspace of the independent variables in which there are two solutions is limited by a boundary on which there is one solution. The choice of  $\omega_3$  and  $\omega_9$  is just one example of the 36 possible ways that the pair of dependent variables can be chosen. In the actual calculation, different choices are made at different stages of the computations for the reasons to be stated in section I-D.

**C. Conformational Energy.** The potential energy of the molecule in a given conformation is computed by summing the nonbonded, electrostatic, and (where applicable) hydrogen bonded terms over all pairs of atoms. The nonbonded energy is expressed as

$$E_{\text{NB}} = \sum_i \sum_{j \neq i} \epsilon_{ij} [(R_{ij}/r_{ij})^{12} - 2(R_{ij}/r_{ij})^6] \quad (14)$$

where  $\epsilon_{ij}$  is the minimum energy (at  $R_{ij}$ ) associated with an interaction between atoms  $i$  and  $j$ , and  $r_{ij}$  is the distance between atoms  $i$  and  $j$ . The parameters  $\epsilon_{ij}$  and  $R_{ij}$  are those derived from studies of crystals of small model compounds.<sup>12</sup> For interactions between atoms separated by three bonds, about only one of which rotation takes place, i.e., so-called 1-4 interactions, the repulsive coefficient is reduced<sup>4</sup> by a factor of 2. The 10-12 hydrogen bond potential described by McGuire et al.<sup>13</sup> is used in place of eq 14 in the case of interactions between atoms capable of participating in hydrogen bonding. This potential is of the form

$$E_{\text{HB}} = \sum_{\text{H-bond pairs}} (A/r^{12}) - (B/r^{10}) \quad (15)$$

where  $r$  is the distance between the hydrogen-bonding atoms. The parameter  $A$  was refined in studies of crystals of small model compounds.<sup>12</sup> The electrostatic energy is expressed as

$$E_{\text{ES}} = 332 \sum_{i,j} \frac{q_i q_j}{D r_{ij}} \quad (16)$$

where the partial atomic charges ( $q_i$  and  $q_j$ ) are those reported elsewhere,<sup>4</sup> and the dielectric constant  $D$  is taken<sup>4</sup> as 2.

Through the third step described in section I-A, these pairwise sums do not include hydrogen atoms explicitly, when they are attached to aromatic or aliphatic carbon atoms. Instead, as an approximation, the CH, CH<sub>2</sub>, and

CH<sub>3</sub> groups were represented by a single "united atom" possessing appropriately enlarged radii and parameters modified in order to reflect the effect of the entire group of atoms. The adjustment of these parameters is described in ref 14. However, for interactions between hydrogen atoms involved in 1-4 type interactions, this approximation is inadequate, and the hydrogens had to be included explicitly. This was accomplished by first computing the total interaction energy in 10° increments in the intervening dihedral angle, for all atom pairs whose relative positions depend only on variation of that dihedral angle. The resulting dependence of energy on dihedral angle was then fit by a 12-term Fourier series (6 terms are sufficient for variation of side-chain dihedral angles). For any given conformation, the hydrogens involved in 1-4 type interactions are treated explicitly by evaluating the appropriate Fourier series; the hydrogens involved in longer-range interactions than 1-4 type were treated by the united atom approximation.

The united atom approximation is used only as a means to reduce the computer time required for energy minimization. In the final stages of refinement (the fourth step), when high-energy minima have been eliminated, the hydrogens are once again treated explicitly.

**D. Minimization of Potential Energy.** The energy minimization was accomplished by means of a line search technique which provides energy minima along lines in hyperspace. The procedure for selecting the lines in hyperspace is a simplified version of the "general partan" method, as described by Scott et al.<sup>15</sup> Without computing gradients, a line is chosen in an arbitrary direction and the minimum along this line is found. A second line is chosen parallel to the first and the minimum along this line is also found. A third line is then constructed by joining these two minima, and the search continues along that line. This completes an iteration in two dimensions. For the seven-dimensional Gr-S backbone, a fourth line parallel to the third is constructed, and the procedure is continued until a seven-dimensional iteration is completed. The lines are initially chosen so that, by the time a search is made along the last line, all the variables are changing simultaneously. Backbones were subjected to three cycles of minimization where one seven-dimensional iteration completes a cycle. As the seven independent variables were changed in a minimization cycle, the symmetry equations were continually solved simultaneously in order to maintain a closed ring with C<sub>2</sub> symmetry throughout the cycle. After each cycle, the dependent variables were reassigned. This was done mainly for two reasons. (a) The minimizer that was used biases the relative importance of the independent variables (e.g., the first variable tends to alter more than the second variable). The changes of independent variables were made to rectify this bias. (b) The minimizer does not perform well in the vicinity of the boundary between the regions where solutions to the symmetry equations do and do not exist. This could be averted by changing the choice of independent variables so that a point near the boundary then appeared well displaced from the new boundary.

During the course of any given line search, regions of ( $\phi, \psi$ ) space may be encountered in which solutions to the C<sub>2</sub> symmetry equations no longer exist. In earlier work using symmetry equations to study cyclohexaglycyl,<sup>16</sup> such an encounter was considered fatal, and the conformation was discarded. In the present study, however, these discontinuities in the energy surface were removed by assigning to a disallowed point a fictitious energy which slightly exceeded that of the previous allowed point. Upon encountering this apparent increase in energy, the line search reversed direction and the search continued into the allowed region.

This minimization technique was used in the early stages of minimization. For the final refinement of the energy, when the united atom approximation was abandoned, the Fletcher–Powell<sup>17</sup> modification of the Davidon<sup>18</sup> minimizer was used.

**E. Selection of Starting Conformations.** As described in section I-B, the backbone is uniquely determined by specification of any seven backbone dihedral angles. Three entirely different selection strategies, referred to as strategy A, B, and C, were used to generate sets of independent variables referred to as A, B1, B2, and C1–C6 in order to ensure adequate sampling of the ( $\phi, \psi$ ) space. These sets of independent variables generated the collection of starting conformations for subsequent energy minimization. The strategy A is a semiempirical method in which available experimental data<sup>19</sup> on Gr-S were used. In the strategies B and C, no experimental data on Gr-S were used. Instead, information derived from theoretical studies on both proteins and small peptides was utilized in order to select values for the independent variables.

**Strategy A.** It has been shown previously<sup>20–22</sup> that the combined use of conformational energy calculations and NMR measurements can resolve ambiguities in both techniques. The ambiguity in the computational method is the existence of many local minima in the energy surface. In the NMR method, the information that can be obtained experimentally is not usually complete enough to specify the conformation uniquely. The relationship between vicinal proton spin–spin coupling constants and the dihedral angle  $\phi$  is not unique, and no direct information can be obtained about the dihedral angle  $\psi$ . The first approach for assigning the independent backbone angles (strategy A) utilizes the relationship<sup>23–25</sup> between the experimentally determined coupling constants  $J_{\text{NH}\alpha\text{H}}$  and the dihedral angles  $\phi_i$ . Four of the nine backbone dihedral angles may be assigned a probable value using these experimental data. If it is assumed (temporarily) that the  $\phi_i$ 's selected in this manner are known exactly and can be fixed, then the problem of selecting reasonable starting conformations in seven-dimensional  $\phi, \psi$  space is reduced to a search in three-dimensional space. A further reduction in the number of variables is achieved by considering the energetic restrictions to variation of the dihedral angle  $\psi$  of Pro. By fixing the value of  $\psi_{\text{Pro}}$ , a total of five dihedral angles can be assumed to be known. It then becomes necessary to search only a two-dimensional conformational space; this can be accomplished easily by using a two-dimensional grid.

The values for the fixed dihedral angles are selected by the following considerations. The large values of  $J_{\text{NH}\alpha\text{H}}$  (8.5–10 Hz) for the residues Val, Orn, and Leu<sup>7,26</sup> indicate that the corresponding  $\phi_i$ 's can be assigned a value of either  $-110^\circ$  or  $-130^\circ$ . The coupling constant for D-Phe has been reported to be 4.1 Hz.<sup>26</sup> The correct assignment for  $\phi$  of D-Phe is more ambiguous, resulting in a choice of four possible values:  $-110^\circ$ ,  $175^\circ$ ,  $70^\circ$ ,  $-10^\circ$ . Taking the  $\phi_i$ 's to be the same for Val, Orn, and Leu, there are thus eight possible combinations of the  $\phi_i$ 's for the sequence Val-Orn-Leu-D-Phe. The value of  $\psi$  for Pro is energetically restricted,<sup>5,27–29</sup> and can be adequately represented by  $-55^\circ$  and  $+120^\circ$ .

As a result of these assignments, there were 16 different ways to fix the invariant dihedral angles, and the entire conformational space accessible to the molecule could be examined by gridding these 16 two-dimensional surfaces. The dihedral angles  $\psi_i$  for Val and Orn were chosen (arbitrarily) as the independent variables to be varied in the gridding procedure. These were varied from  $-180^\circ$  to  $+180^\circ$  in  $30^\circ$  increments and, at each point, the two dependent variables were computed from equations analogous to eq A-11, A-15, and A-16. These equations provided either no

**Table I**  
Dihedral Angles<sup>a</sup> Comprising Independent  
Variable Set B1

Val		Orn		Leu		Pro
$\phi$	$\psi$	$\phi$	$\psi$	$\phi$	$\psi$	$\psi$
-83	98	-83	83	-86	81	-60
-153	144	-150	133	-151	136	-40
-74	142	-73	152	-81	-57	-20
-80	-56	58	66	-154	-66	70
56	74	-154	-64	61	65	90
-72	-34	-72	-55	-149	99	110
33	64					160
71	-74					

<sup>a</sup> The values of  $\phi$  and  $\psi$  for each residue were taken as a pair.

solutions or two solutions (and, in rare cases, only one solution). The regions in which there were no solutions corresponded to asymmetric-ring or open-ring conformations, and were no longer of interest. The area in which solutions did exist consisted of two branches: one was determined by the upper signs in eq A-11, and the other by the lower signs. As a result, each of the 16 two-dimensional grids spanned 32 different surfaces in closed-symmetric ring-conformational space. For each point on these surfaces, the conformational energy was computed so that the gridding could be represented by energy contour maps. In this manner, the entire conformational energy surface of the molecule was represented by 32 energy contour maps. All local energy minima were located, and a representative point from each was selected for subsequent energy minimization in which the invariant angles were now allowed to vary (with simultaneous solution of the symmetry equations). An illustration of one of the 32 energy contour maps is provided in section I-F.

Each of the 32 conformational energy maps sampled  $12 \times 12 = 144$  points in independent-variable space; eight of the maps were refined by computing 144 additional points by frame shifting the grid by  $15^\circ$ . By this procedure, 5760 sets of independent variables were examined.

**Strategy B.** Strategy A was limited by the fact that the relationships between  $\phi$  and  $J_{\text{NHCOH}}$  have not been established unambiguously. Furthermore, it is possible that the observed coupling constants do not correspond to a single conformation but, instead, represent average values arising from a number of rapidly interconverting conformations. Therefore, additional starting conformations were generated from a theoretical rather than from an experimental point of view. The strategy here was to assume that the overall structure of Gr-S is determined by the conformational states accessible to the individual amino acid residues of which the molecule is comprised. Likely values for  $(\phi, \psi)$  pairs were taken from the conformational energy analysis of *N*-acetyl-*N'*-methylamino acid amides carried out by Lewis et al.<sup>5</sup> to obtain the independent variable set B1. These are listed in Table I. The two remaining variables ( $\phi_{\text{Phe}}$ ,  $\psi_{\text{Phe}}$ ) were taken as the dependent variables. Although the choice of which variables are to be taken as dependent is arbitrary, there is evidence<sup>30</sup> that the closure of the ring at Phe may occur during the biosynthesis of this antibiotic. In particular, it was shown that the biosynthesis of Gr-S is accomplished by dimerization of two identical pentapeptides (D-Phe-Pro-Val-Orn-Leu) which are linked by a sulfhydryl bond to the enzyme surface at the Leu end.<sup>30</sup> When taken in all combinations, the dihedral angles listed in Table I generated 2016 seven-variable combinations.

**Table II**  
Dihedral Angles<sup>a</sup> Comprising Independent  
Variable Set B2

Val		Orn		Leu		Pro
$\phi$	$\psi$	$\phi$	$\psi$	$\phi$	$\psi$	$\psi$
-120	160	-100	135	-100	100	-20
-85	135	-100	40	-80	140	-50
-80	115	-60	-10	-40	-20	120
-65	-10	-60	120	-130	160	150
-40	-50	-40	-35	-40	-45	
-150	170	65	45			
		-150	170			

<sup>a</sup> The values of  $\phi$  and  $\psi$  for each residue were taken as a pair.

**Table III**  
Types of Bends<sup>a</sup>

Type	$\phi_{i+1}$ , deg	$\psi_{i+1}$ , deg	$\phi_{i+2}$ , deg	$\psi_{i+2}$ , deg
I	-60	-30	-90	0
I'	60	30	90	0
II	-60	120	80	0
II'	60	-120	-80	0
III	-60	-30	-60	-30
III'	60	30	60	30

<sup>a</sup> The dihedral angles were given by Venkatachalam<sup>32</sup> as approximate values for the respective bends type I through type III' inclusive.

This collection of  $(\phi, \psi)$  pairs chosen for individual amino acids was expanded further (to create independent variable set B2) by considering data from frequencies of occurrence for  $(\phi, \psi)$  pairs as compiled by Burgess et al.<sup>31</sup> In that study, the collection of proteins whose structures are known by X-ray crystallography was examined, and the number of times that each residue exhibited a particular conformation was tabulated on a  $\phi, \psi$  map. From these maps, local conformations found frequently in proteins were chosen as points to consider in the Gr-S study. The  $(\phi, \psi)$  pairs taken are listed in Table II and, when considered in all combinations, provide 840 additional independent variable sets.

**Strategy C.** The fact that Gr-S is a cyclic molecule implies that a  $\beta$  bend may be present to accomplish the chain reversals. The strategies A and B do not adequately sample the region of  $(\phi, \psi)$  space in which dihedral angles producing  $\beta$  turns are found. Two-residue sequences produce a chain reversal provided that the four dihedral angles (referred to as  $\phi_{i+1}$ ,  $\psi_{i+1}$ ,  $\phi_{i+2}$ ,  $\psi_{i+2}$ <sup>32</sup>) of these residues have values approximating those listed in Table III. In Gr-S there are five unique positions (corresponding to the existence of five unique dipeptide sequences) where a  $\beta$  turn can be formed. These possible sequences are Orn-Leu, Leu-D-Phe, D-Phe-Pro, Pro-Val, and Val-Orn. Specification of the dihedral angles  $\phi_{i+1}$ ,  $\psi_{i+1}$ ,  $\phi_{i+2}$ ,  $\psi_{i+2}$  for each dipeptide sequence determines four of the seven dihedral angles required to generate a backbone. Thus, by fixing a  $\beta$  bend at one of these five positions, only three additional dihedral angles need to be specified in order to generate a backbone molecule. (In the case in which Pro is located within the bend sequence, the angles  $\phi_{i+1}$ ,  $\psi_{i+1}$ ,  $\phi_{i+2}$ , and  $\psi_{i+2}$  can be used to specify only three of the seven independent variables.) To generate conformations containing  $\beta$  turns, appropriate sequences of four (or three) of the seven independent variables were assigned values taken from Table III. For the remaining three (or four) variables,  $(\phi, \psi)$  pairs were selected from the  $\epsilon$  (extended) region of a  $(\phi, \psi)$

Table IV  
Independent Variables<sup>a</sup> to Construct  $\beta$  Bend at Orn-Leu

Val		Orn		Leu		Pro
$\phi$	$\psi$	$\phi$	$\psi$	$\phi$	$\psi$	$\psi$
-83	98	-60	-30	-90	0	-60
-153	144	-60	120	80	0	-50
-137	156	-60	-30	-60	-30	-40
-74	142					-30
-80	-56					-20
56	74					70
-72	-34					80
71	-74					90
33	64					120
-150	150					140
-120	150					
-150	120					
-120	120					
-170	150					

<sup>a</sup> The values of  $\phi$  and  $\psi$  for Val were taken as a pair; those for Orn and Leu (on a given line) were taken as a set.

map for *N*-acetyl-*N'*-methyl-L-alanyl-L-alanine.<sup>5</sup> In addition, other ( $\phi, \psi$ ) pairs of high statistical weight were sampled.<sup>5</sup> For the dipeptide sequences Orn-Leu, Pro-Val, and Val-Orn, only bends of types I, II, and III were considered. The decision to neglect the types I', II', and III' bends was based on the result of calculations<sup>33</sup> on various dipeptide sequences, which indicate that, for most of the dipeptide species, types I', II', and III' bends do not appear as energy minima. (Types I, II, and III are indeed observed to occur much more frequently in proteins than types I', II', or III'.) In the cases of the dipeptides Leu-D-Phe and D-Phe-Pro, in which a D-type residue is involved, the above argument for neglecting types I', II', and III' bends may not be applicable. Therefore, for these cases, all possible bend types should be considered. However, D-Phe-Pro is restricted to three choices (I, II', and III) because  $\phi$  of Pro is fixed at  $-75^\circ$ . In the case of Leu-D-Phe, all possible bends are highly destabilized by the adjacent proline residue at position  $i + 3$ . The pyrrolidine ring projects into the interior of the bend, thereby making such conformations sterically impossible. This situation does not change even when types I', II', and III' bends are included; thus, we consider only types I, II, and III for Leu-D-Phe. A representative example showing the choice of independent variables for the case of a bend at the sequence Orn-Leu is given in Table IV. When taken in all combinations, these selected dihedral angles sample a total of 420 points in independent variable space and comprise set C1. In a similar way independent variable sets C2–C5 containing 420, 448, 264, and 333 points, respectively, were generated for bends at the remaining dipeptide sequences.

If the dihedral angles of residues adjacent to a  $\beta$  bend, viz., the  $i$ th and  $(i + 3)$ th residues, are restricted to particular values, a four-residue sequence stabilized by two transannular hydrogen bonds is generated. This specific local conformation is not considered explicitly in the bend-generating processes described above. The set of independent variables was, therefore, expanded in order to include this special local conformation. The dihedral angles required to produce such a structure were taken from Table 3 of ref 22, where they were found to create this local conformation in oxytocin. These dihedral angles were permuted around the molecule in order to create a bend at each of the five allowed positions. For cases in which the fixed  $\phi$  of proline disrupts this sequence, an attempt was made to compen-

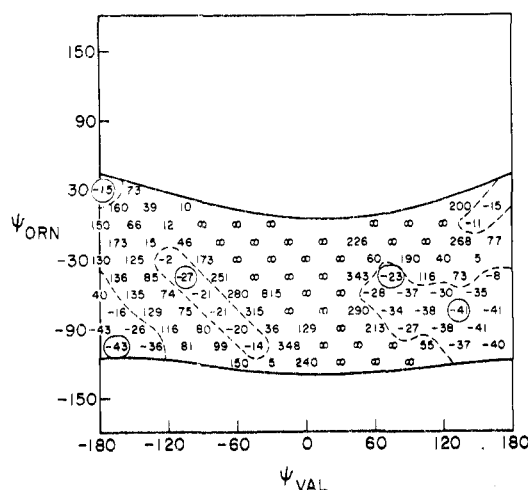


Figure 2. A representative conformational energy map illustrating the variation in energy with  $\psi$  of Val and  $\psi$  of Orn while holding the remaining dihedral angles fixed as described in the text. The solid lines bound the regions in which solutions to the  $C_2$  symmetry equations do and do not exist. At each point within the allowed region, the corresponding energy is given, in kcal/mol, or is represented by the symbol  $\infty$  where the energy exceeds 1000 kcal/mol. The dashed lines enclose low-energy regions from which the circled points were taken for energy minimization.

sate by adjusting the adjacent dihedral angles (using molecular models) in order to preserve the structure. Thus, 40 additional points were chosen which comprise set C6.

The total number of independent variable sets considered by the combined strategies C1–C6 is 1925.

**F. Reduction of Number of Backbone Conformations by Classification, Grouping, and Energy Minimization.** A total of 10,541 points in independent variable space, as chosen by strategies A, B, and C, were sampled. For each point, two solutions to the symmetry equations may exist thereby generating possibly twice that number of actual conformations. However, solutions were found to exist in only about half of the cases. Therefore, a total of approximately 10,000 conformations actually were generated. Limited available computer time prohibited execution of energy minimization on each of these. Therefore, in this section, the procedures for reducing the sample size prior to energy minimization are presented. Two procedures were used, for reasons indicated below: one is applied to conformations generated by strategy A, and the other is applied to those generated by strategies B and C.

In the case of strategy A, the reduction was achieved simply by choosing from each of the conformational energy maps one or a few conformations to represent each of the local minima having energy less than 0.0 kcal/mol; i.e., local minima with positive energies were not sampled. A representative example of one of these maps arising from one choice of  $\phi_i$  for Val, Orn, Leu, and Phe and  $\psi$  of Pro is shown in Figure 2. Five points were selected from this particular map for subsequent energy minimization with respect to all independent variables, with simultaneous solution of the symmetry equations. Additional points (making a total of 64) were selected from the remaining 31 maps (not shown here). The initial energies, before minimization, ranged from  $-48$  to  $0.0$  kcal/mol. Within the framework of strategy A, these 64 points represent all of the low-energy local minima of the molecule, and the reduction of the initial sample size from 5760 conformations to 64 is, therefore, justified.

The strategies B and C produced 1040 and 872 cases, respectively, satisfying the symmetry equations which, be-



cause of the doubling of solutions, generated 3824 conformations. In contrast to the gridding procedure of strategy A (which provided information about the *shape* of the energy surface near local minima), strategies B and C sampled only isolated points in conformation space (and thus provided no information about the shape of the energy surface near local minima). Therefore, different arguments had to be used to justify the selection of a few of these for subsequent energy minimization. We began by classifying conformations according to their energies, and proceeded to group them by this criterion. The energies of the initially generated conformations ranged from  $-48.3$  to  $>10^{10}$  kcal/mol. These conformations were arranged in three categories according to energy. The first category consisted of 139 conformations having very low energy (less than  $-30$  kcal/mol and greater than  $-48.3$  kcal/mol). It was assumed that energies in this range indicate the proximity of a sampled point to a minimum in the potential energy surface. All conformations in this energy range were taken for subsequent energy minimization. The second category contained the 606 conformations found in the energy range between  $-30$  and  $185$  kcal/mol. This set of conformations was sorted, and conformations not differing by more than  $20^\circ$  in each dihedral angle (both independent and dependent) were grouped together. One representative conformation from each of the 106 resulting groups was then subjected to subsequent energy minimization. By this procedure the 606 conformations were reduced to 106. The remaining 3079 conformations having energies exceeding  $185$  kcal/mol formed the third category. Subsequent energy minimizations were not carried out for these high-energy conformations because it was judged that they were likely to become trapped in high-energy local minima even when energy minimization was applied. This judgment was supported by the following two observations. First, it was observed that those starting conformations in category 2 which had high initial energies rarely reached a low-energy local minimum. Additional evidence was obtained by examining a subset of conformations from B1 in a modified way. Using the upper five ( $\phi, \psi$ ) pairs in Table I for each of the residues Val, Orn, and Leu with two values ( $-55$  and  $120^\circ$ ) for  $\psi$  of Pro, a subset of B1 was generated. From the 250 possible combinations of these dihedral angles 127 independent variable sets had solutions to the symmetry equations, thus generating 254 conformations. The energies of these ranged from  $-46$  to  $10^{14}$  kcal/mol. All 254 were subjected to energy minimization using the minimization technique described in section I-D, slightly modified as follows: in this version, energy minimization was terminated upon an encounter with the boundary. The few low-energy minima obtained in this search were the same as those obtained by using the cut-off criteria as described above, and, as expected, the high-energy starting conformations either reached a high-energy local minimum or encountered the boundary and were discarded. These observations indicate that high-energy conformations can be discarded at the outset without risking overlooking a significant low-energy minimum. Therefore, the conformations of category 3 could be discarded safely.

Employing these reduction methods, a total of 309 conformations was left for subsequent energy minimization, all in the energy range between  $-48$  and  $+185$  kcal/mol.

**G. Energy Minimization of Backbone Molecule.** The 309 backbone molecules derived from the selection process described above were subjected to three cycles of energy minimization using the "general partan" procedure described in section I-D. These 309 conformations merged into 223 unique minima with energies ranging from  $-56$  to  $+150$  kcal/mol. Of these, 12 had energies greater than 10

kcal/mol and were discarded. The remaining 211 were retained for construction of full molecules (molecules with side chains included).

**H. Energy Minimization of Full Molecules.** The set of energy-minimized backbones was converted next to full molecules by including the side chains. This required specification of 9 additional degrees of freedom when the united atom approximation was used and 13 in the full-atom treatment. The dihedral angles  $\chi^2$  and  $\chi^3$  of Orn were taken initially as  $180^\circ$  (extended), and  $\chi^2$  of Phe and  $\chi^4$  of Orn were set at  $90^\circ$ . The remaining five dihedral angles ( $\chi^1$  of Val, Orn, Leu, and Phe, and  $\chi^2$  of Leu) were varied systematically through values chosen to represent the minima in the rotational energy about these bonds. These values are  $-60$ ,  $60$ , and  $180^\circ$ . Using these values, there were  $3^5 = 243$  possible side-chain conformations which could be chosen for each of the 211 low-energy backbones. In order to select the best side chain starting conformation for each low-energy backbone, the initial energy (before minimization) of the *whole* molecule was determined for each of the 243 combinations of side-chain variables. The combination giving the lowest energy was selected as the starting side-chain conformation for minimization of the energy of the whole molecule, using the united atom approximation. The total united atom energy of the full molecules constructed in this way was then minimized by a two-step process. First the energy was minimized with respect to side-chain variables while maintaining a fixed backbone. Then the full molecule was subjected to energy minimization with respect to all independent variables (with simultaneous solution of the symmetry equations).

Following the step of conversion to full molecules (side chain energy minimization on fixed backbones), the resulting energies range from  $-23$  to  $7207$  kcal/mol. This range was reduced to  $-28.3$  to  $976$  kcal/mol upon subsequent energy minimization with respect to all dihedral angles. Of the 211 minimum energy backbones sampled, 128 were found to yield full molecules with negative conformational energies.

**I. Final Refinement.** The 128 conformations with negative energies were sorted, and those conformations differing by  $\leq 20^\circ$  in all backbone dihedral angles were grouped together. Many conformations were found to be unique, and this classification resulted in 78 groups, each containing from one to five members. By applying the same criterion to the side-chain dihedral angles, the conformations within each individual group were reclassified into subgroups. The resulting 97 subgroups represent unique local minimum-energy conformations. Attention was focused on the 59 conformations (41 subgroups) whose energies varied continuously in the range of  $-28.3$  to  $-14.2$  kcal/mol. These conformations were found to have widely separated energies when hydrogens were included explicitly in the calculation of the potential energy. The atomic interactions responsible for these energy changes consisted almost exclusively of interactions between side chains which had been allowed to pack too closely in the united atom approximation. The final energy minimizations, therefore, were confined to the independent variables of only the side chains.

A representative member of each of the 41 subgroups found within 14 kcal of the lowest united atom minimum-energy conformation was subjected to a final minimization using the Fletcher-Powell minimization technique to vary the side-chain dihedral angles. The initial conformations of side-chain methyl groups were taken as  $\chi = 60^\circ$ . In every case, only small adjustments (less than  $20^\circ$ ) in dihedral angle were required to reach a new energy minimum, thus indicating that the minima reached under the united atom



Table V  
β-Pleated Sheet-Type Minima

	Dihedral angle, deg	M1	M2	M3
Val	φ	-90	-91	-97
	ψ	100	101	127
Orn	φ	-127	-123	-80
	ψ	125	124	113
Leu	φ	-156	-152	-106
	ψ	117	114	95
D-Phe	φ	60	59	92
	ψ	-137	-137	-148
Pro	φ	-75	-75	-75
	ψ	-18	-13	-36
Val	χ <sup>1</sup>	178	178	176
	χ <sup>2,1</sup>	51	50	51
	χ <sup>2,2</sup>	69	68	67
Orn	χ <sup>1</sup>	-63	-72	174
	χ <sup>2</sup>	-170	145	160
	χ <sup>3</sup>	-177	178	-174
	χ <sup>4</sup>	25	66	78
Leu	χ <sup>1</sup>	-179	-177	-61
	χ <sup>2</sup>	72	75	154
	χ <sup>3,1</sup>	53	57	55
	χ <sup>3,2</sup>	61	62	58
D-Phe	χ <sup>1</sup>	179	178	60
	χ <sup>2</sup>	-91	89	74
Energy, kcal/mol		-14.4	-12.3	-12.2

approximation are located very near the energy minima of the full-atom potential. The final energies (on the full-atom energy scale) ranged from -14 to +56 kcal. The 56 additional subgroups of united atom minima having energies exceeding that of the lowest by more than 14 kcal were not subjected to this final refinement process, since it was judged that an energy of this magnitude could not be reduced to that at the global minimum when all hydrogens were included.

## II. Results

**A. Classification of Minimum Energy Conformations and Their Mutual Relationships.** The dihedral angles and energies of the nine most stable minimum energy conformations (MEC's) are listed in Tables V and VI. Of these, three (M1–M3) are at least 8 kcal/mol more stable than the remaining ones. These three have very similar backbone conformations and can be considered to be members of the same class (GM1). The MEC's M4 and M5 comprise a second class (GM2). It is possible to obtain the class GM1 from GM2 by a very simple operation. In general, by varying a given  $\psi_i, \phi_{i+1}$  pair, the intervening peptide group can be rotated while leaving the overall shape of the molecule essentially unchanged. The first class GM1 can be converted to GM2 by such an operation, i.e., by rotating the peptide group (by approximately 180°) between the residues Leu and Phe.

In the class GM1, the residues Val, Orn, and Leu are in the extended conformation and form a structural variant of the classical antiparallel β-pleated sheet. The two chains are linked at the ends by a β turn at the sequence D-Phe-Pro. The conversion from GM1 to GM2 disrupts the pattern of hydrogen bonding found in GM1, and thus destabilizes the class GM2. However, even in the absence of hydrogen bonding, the class GM2 is energetically more stable than M6, M7, . . . , which have distinctly different molecular conformations than M1–M5. The fact that the two classes of lowest energy conformations are related to each

Table VI  
Higher Energy Minima

	Dihedral angle, deg	M4	M5	M6	M7	M8	M9
Val	φ	-131	-132	-95	73	-153	-147
	ψ	161	163	-56	-83	145	146
Orn	φ	-143	-142	-74	-64	177	-88
	ψ	152	152	149	143	176	-47
Leu	φ	-94	-94	-164	-158	-149	-165
	ψ	-25	-20	147	120	142	138
D-Phe	φ	152	146	143	134	149	93
	ψ	-82	-82	-160	-71	-163	-157
Pro	φ	-75	-75	-75	-75	-75	-75
	ψ	-24	-25	-41	86	-43	168
Val	χ <sup>1</sup>	-68	-65	-177	178	71	74
	χ <sup>2,1</sup>	69	70	54	70	71	74
	χ <sup>2,2</sup>	47	50	66	51	51	70
Orn	χ <sup>1</sup>	72	66	-76	-75	-113	72
	χ <sup>2</sup>	-170	178	-179	176	146	-176
	χ <sup>3</sup>	-171	-171	179	166	166	-177
	χ <sup>4</sup>	91	84	85	66	93	92
Leu	χ <sup>1</sup>	-164	-61	-155	62	-168	-177
	χ <sup>2</sup>	87	154	77	108	73	72
	χ <sup>3,1</sup>	68	56	43	55	51	53
	χ <sup>3,2</sup>	65	57	68	58	60	61
D-Phe	χ <sup>1</sup>	180	85	72	170	80	-97
	χ <sup>2</sup>	117	86	73	98	58	81
Energy, kcal/mol		-4.28	-2.6	1.5	4.0	8.8	11.6

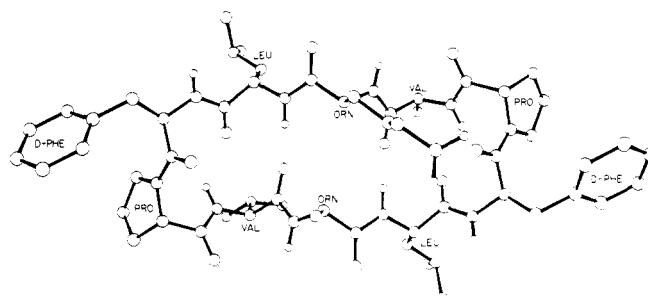


Figure 3. A view of minimum energy conformation M1 looking down the  $C_2$  symmetry axis. For clarity, one ornithine and one valine side chain have been deleted. Dashed lines denote hydrogen bonds.

other by minor conformational changes implies that, in this particular molecule of (Val-Orn-Leu-D-Phe-Pro)<sub>2</sub> with  $C_2$  symmetry, there is a conformational subspace in which the conformational energy is distinctly low and in which the two classes GM1 and GM2 exist. (It should be noted that we have reached this particular subspace five times, i.e., M1–M5, but we have never been led to other subspaces with distinctly low energy. If there were any other subspaces with as distinctly low energy as the one containing M1–M5, it is reasonable to expect that we would have been led to each of them at least once.) Therefore, it can be concluded with some confidence that the lowest energy conformation obtained in this study is in fact the global minimum.

**B. Conformational Features of GM1. 1. Comparison of GM1 with Experimental Data.** A view of M1 down the twofold axis of symmetry and a stereo illustration are shown in Figures 3 and 4, respectively. Since M1, M2, and M3 are so closely related in backbone conformation, these figures illustrate the general backbone of M2 and M3 as

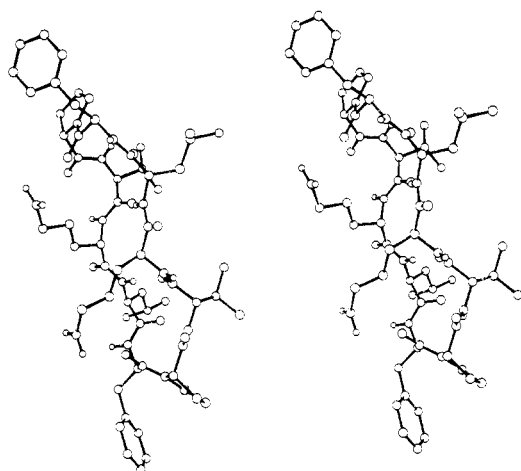


Figure 4. A stereoscopic illustration of minimum-energy conformation M1.

well as M1. The three models differ mainly in the orientations of the side chains.

The backbone dihedral angles of all three are completely consistent with experimental data. From Karplus-Bystrov<sup>25</sup> curves depicting the variation in the vicinal coupling constant  $J_{\text{NHC}^{\alpha}\text{H}}$  with the dihedral angle  $\phi$ , the  $\phi_i$ 's of M1 ( $-90$ ,  $-127$ , and  $-156^\circ$ ) correspond to coupling constants in the ranges 8.3 to 9.4 Hz, 9.8 to 11.2 Hz, and 7.5 to 8.5 Hz. Each is consistent with the reported range of 8.5 to 10.0 Hz.<sup>7,26</sup> Likewise,  $\phi = 60^\circ$  of Phe implies a coupling constant in the range 3.5 to 4.3 Hz, and the reported value is 4.1 Hz.<sup>26</sup> The values of  $\phi_i$  for M2 and M3 also agree with experiment.

The exchange rates of each amide proton in Gr-S have been measured by following the rate of disappearance of the NMR signal for each proton undergoing exchange with deuterium.<sup>7,26</sup> These rates have been measured independently by following the rate of escape of tritium through a dialysis membrane.<sup>34</sup> These experiments show that the amide protons of Val and Leu exchange much more slowly than those of Phe or Orn. These slowly exchanging protons are believed to be either sterically shielded from solvent or involved in hydrogen bonds. Additional evidence that the amide protons are involved in hydrogen bonding is provided by measurements of the temperature dependence of chemical shifts. The amide protons corresponding to Val and Leu have very small temperature coefficients whereas amide protons for Phe and Orn have temperature coefficients similar to that of a model compound which cannot form hydrogen bonds.<sup>35</sup> It is concluded from the above experiments that the amide protons of both Val and Leu are involved in intramolecular hydrogen bonds. In models M1-M3, the amide hydrogens of both Val and Leu are located in the interior of the decapeptide ring. The protons of both residues are, therefore, relatively inaccessible to solvent. If it is assumed that a significant  $\text{N-H}\cdots\text{O}$  hydrogen bond is characterized by a near-linear arrangement of the  $\text{N-H}\cdots\text{O}$  atoms with the distance  $r_{\text{NH}\cdots\text{O}}$  not exceeding 3.2 Å, then only the NH of Leu participates in a formal hydrogen bond ( $r_{\text{NH}\cdots\text{O}} = 2.88$  Å). For the interactions between Val NH and Leu CO, this distance is 3.6 Å and, therefore, this interaction can be classified only as a very weak hydrogen bond. The slow exchange rates for the amide protons of both Leu and Val are more likely a consequence of weak hydrogen bonding accompanied by inaccessibility to solvent.

Although the quantity of experimental data concerning side chains is much more limited than that of the back-

bone, there are a few points worth noting. All three models (M1 to M3) have the same valine conformation (i.e.,  $\chi^1 \approx 180^\circ$ ). This value of  $\chi^1$  has been predicted by Gibbons et al.<sup>20,36</sup> who observed a large coupling constant ( $J_{\text{C}^{\alpha}\text{HC}^{\beta}\text{H}} = 8.6$  Hz) for Val which is not temperature dependent. This is interpreted<sup>19b</sup> to mean that the side chain is "likely" to be frozen in a conformation close to trans. They also reported that Leu "appears to be frozen" while, in the side chains Orn and Phe, "some free rotation is apparently occurring". The conformation of Leu in M3 differs from that in M1 and M2. This indicates that Leu can exist in two rotational states; hence, our results do not agree with their prediction concerning the behavior of Leu. Our three models (M1, M2, and M3) do, however, suggest that the residues Orn and Phe can occupy more than one rotational state. In models M1 and M2, the phenylalanine side chain is oriented in such a way as to place the plane of the aromatic ring over the  $\delta\text{-CH}_2$  group of the neighboring proline residue. In this orientation the magnetic anisotropy of the aromatic ring should cause the chemical shifts of the  $\delta\text{-CH}_2$  protons to move upfield by  $\sim 0.8$  to 1.0 ppm from the usual position of  $\sim 3.6$  ppm. This effect has been observed in cyclosymmetric hexapeptides containing the repeating sequence  $(\text{-L-XXX-D-Phe-L-Pro})_2$  where XXX = Ala, Orn, or His.<sup>37</sup> In these hexapeptides, the proposed backbone conformation of the sequence D-Phe-Pro is very close to that found in M1 and M2. Two complete 300-MHz NMR spectra of Gramicidin S have been published (Figure 32a of ref 19b), one at  $20^\circ\text{C}$ , the other at  $60^\circ\text{C}$ . In the  $20^\circ\text{C}$  spectrum two resonances have been assigned to the  $\delta\text{-CH}_2$  protons of Pro. One of these appears at  $\sim 3.6$  ppm and corresponds to the normally observed chemical shift for these protons. The other peak in the  $20^\circ\text{C}$  spectrum assigned to  $\delta\text{-CH}_2$  of Pro appears at 2.6 ppm where it is obscured by the solvent  $\text{DMSO-}d_6$  resonance. As the temperature is increased to  $60^\circ\text{C}$  the peak at 3.6 ppm is shifted  $\sim 0.05$  ppm downfield while the signal at 2.6 undergoes a greater downfield shift to  $\sim 2.8$  ppm. The existence of the resonance at 2.6 to 2.8 ppm at both temperatures clearly indicates that the phenylalanine side chain possesses the conformation predicted by models M1 and M2 in which the aromatic ring is oriented in such a way as to magnetically shield one of the  $\delta\text{-CH}_2$  protons of Pro. The fact that the resonance of this shielded proton has a much greater temperature dependence than that of the unshielded proton at 3.6 ppm suggests that the phenylalanine side chain can occupy at least one additional rotational state in which the aromatic ring is no longer capable of shielding the  $\delta\text{-CH}_2$  protons of Pro. The populations of any additional states increase with increasing temperature.

The ornithine side chain, as well, may be free to occupy more than one rotational state. The model M1 for example is stabilized by a hydrogen bond between a  $\delta\text{-NH}_2$  proton of Orn and the backbone CO of Phe. This hydrogen-bonding contribution to the total energy is sufficient to account for the fact that M1 is  $\sim 2$  kcal/mol more stable than M2 or M3. There is no experimental evidence indicating the existence of this interaction, and it is likely to be highly dependent upon solvent conditions.

The other MEC's obtained in this study do not agree with experimental data as completely as do the models M1-M3.

**2. Influence of Short-Range Interactions in Stabilization of GM1.** Considerable attention has been focused recently on the influence of the side chain of an amino acid residue in determining the conformation of its own backbone.<sup>38</sup> It has been demonstrated<sup>38</sup> that these *intra*-residue interactions play a dominant role in determining conformation in polypeptides and proteins. However, in a ring struc-

ture such as Gr-S, the conditions for ring closure might be expected to predominate, so that individual intra-residue interactions might be sacrificed to some extent in order to minimize the energy of the entire molecule. In this study, however, we find that, in spite of possible constraints imposed by ring closure, the individual residues of Gr-S continue to occupy regions of  $\phi, \psi$  space which correspond to energy minima of individual amino acid residues. Comparing the conformations of the individual residues in Gr-S with the minimum-energy ones for single residues, predicted by Lewis et al.,<sup>5</sup> the backbone and side-chain dihedral angles of Val in M1 are identical with those of the single-residue conformation predicted<sup>5</sup> to have the highest statistical weight. Furthermore, the residues Leu and D-Phe differ by only 20° in one dihedral angle from the predicted single-residue minima of highest and second highest statistical weight, respectively. (In the case of D-Phe, the L-residue minima were converted to those of a D residue by changing the signs of  $\phi$  and  $\psi$ .) Although Orn was not considered in the study of individual residues,<sup>5</sup> the backbone dihedral angles of Orn found in Gr-S are similar to those predicted<sup>5</sup> for a Lys residue. Finally, the dihedral angle  $\psi$  of Pro found in M1 is well within a potential energy minimum found for *N*-acetyl-*N'*-methyl-L-prolineamide. Thus, it appears that short-range interactions also play a dominant role in this cyclic decapeptide.

### C. Comparison with Previously Predicted Models.

The conformations M1–M3 obtained in this study can be classified as a variant of the antiparallel  $\beta$ -pleated sheet type as proposed originally by Hodgkin and Oughton<sup>39</sup> and independently by Schwyzer.<sup>40,41</sup> That model consists of two antiparallel tetrapeptide chains –Val-Orn-Leu-D-Phe–linked at the ends by means of the proline residue, and stabilized by four intramolecular hydrogen bonds between the NH and CO groups of the Val and Leu residues. While the experimental results cited in the previous section strongly support this model, none has the power to predict the exact values for each dihedral angle. Therefore, a number of variations of this model have appeared in the recent literature. Using NMR data providing information on the values of  $\phi$  for Val, Orn, and Leu, Stern et al.<sup>7</sup> predicted a model (SGC) in which the pleated sheet segments are joined by a  $\beta$  turn of type III. Using empirical energy calculations, Mooney et al.<sup>42</sup> derived a similar model (their GSV). (The similarity between GSV and SGC becomes more pronounced following energy minimization of SGC.) A second variation (OV), in which the  $\beta$ -sheet segments are joined by a type II' rather than a type III bend, has been predicted by Ovchinnikov et al.<sup>26</sup> from an analysis of infrared spectra and additional experimental NMR data concerning the dihedral angle  $\phi$  of Phe. A closely related model (DL), also with a type II' bend, has been derived by De Santis and Liquori<sup>43</sup> in a study using a combination of experimental data and empirical energy calculations. The class GM1 derived in this study corresponds to the latter type, i.e., the  $\beta$  bend corresponds to a type II' rather than a type III. In order to compare all previously predicted models with the one proposed here, each of the published structures was subjected to the same series of energy minimizations as described in section I, using the published dihedral angles as starting conformations. (Side-chain dihedral angles not specified were selected as in section I-H.) The resulting conformations, minimized from OV and DL, are shown in Table VII. Each has low energy and reached the same minimum energy conformation (cf. X1, X2, and X3), which in turn is very much like M1–M3. Neither of the models GSV or SGC, however, reached a low-energy minimum. Instead, they became trapped in a local minimum with energy 56 kcal/mol. The high energy can be attributed to the fact

Table VII  
 $\beta$ -Pleated Sheet-Type Minima Derived from  
Previously Published Models

	Dihedral angle	DL <sup>a</sup>	X1 <sup>b</sup>	DL <sup>a</sup>	X2 <sup>b</sup>	X3 <sup>c</sup>
Val	$\phi$	–82	–87	–82	–91	–87
	$\psi$	137	127	137	129	122
Orn	$\phi$	–132	–148	–132	–138	–143
	$\psi$	142	126	142	126	130
Leu	$\phi$	–143	–151	–143	–138	–159
	$\psi$	82	110	82	103	116
D-Phe	$\phi$	58	71	58	71	64
	$\psi$	–116	–140	–116	–139	–139
Pro	$\phi$	–68	–75	–68	–75	–75
	$\psi$	–31	–18	–31	–15	–17
Val	$\chi^1$	180	175	180	175	175
	$\chi^{2,1}$		49		50	49
	$\chi^{2,2}$		65		66	65
Orn	$\chi^1$	–70	–66	–160	177	–69
	$\chi^2$	180	–171	180	176	–171
	$\chi^3$		166		–164	173
	$\chi^4$		50		143	48
Leu	$\chi^1$	–160	–176	–80	–85	178
	$\chi^2$	80	76	160	151	66
	$\chi^{3,1}$		58		54	49
	$\chi^{3,2}$		63		51	62
D-Phe	$\chi^1$	180	175	70	63	177
	$\chi^2$	–80	–92	89	70	–91
Energy, kcal/mol			–8.6		–8.6	–11.2

<sup>a</sup> Unminimized model as published.<sup>43</sup> These authors reported two conformations, having identical backbone but different side-chain conformations. <sup>b</sup> Minimized from <sup>a</sup> after adding the unspecified dihedral angles. <sup>c</sup> Minimized from Ovchinnikov model.<sup>26</sup>

that these models contain a type III  $\beta$  turn rather than type II', even though the GSV and SGC conformations resemble M1 rather closely. Empirical energy calculations on stabilities of  $\beta$  bends<sup>33</sup> have shown that, for the sequence Gly-Pro (a system similar to D-Phe-Pro), bends of type II' and III are energy minima while type I' is not; of the two minima, type II' is at least ten times more stable than type III.

The empirical energy calculations carried out on hairpin turns by Chandrasekaran et al.<sup>44</sup> have demonstrated that an energy minimum for a D-L sequence in a bend corresponds to a conformation near a type II' bend. The conformation corresponding to a type III bend does not appear in their results.

When all previously published conformations<sup>7,15,26,42,43,45,46</sup> were taken as starting conformations, many high- but only one low-energy minimum was obtained. This low-energy conformation was found to be identical with conformations M1–M3 derived independently in this study. Conformation M1 was derived from a starting conformation contained in the independent variable set B1 obtained from a consideration of individual amino acid residue minima. Conformation M2, on the other hand, originated from the set A based on an examination of NMR data. The conformational space identified as GM1, therefore, has been reached by means of at least four different pathways. These are: the refinement of the De Santis-Liquori model,<sup>43</sup> minimization of the energy of the conformation proposed by Ovchinnikov et al.,<sup>26</sup> minimization of the energy of a conformation chosen by strategy B1, and minimization of the energy of a conformation from set A. These starting conformations were all unique (by the crite-

Table VIII  
Coordinates of Structure M1<sup>a,b</sup>

RESIDUE	ATOM	X	Y	Z
L-LEU	N	0.985	-2.752	-0.946
	HN	1.355	-1.833	-1.081
	CA	1.894	-3.836	-1.280
	HA	1.763	-4.557	-0.599
	CB	1.540	-4.431	-2.644
	C*	3.336	-3.334	-1.183
	O	3.735	-2.436	-1.923
	HB	0.500	-4.757	-2.617
	HB	1.607	-3.641	-3.392
	CG	2.402	-5.608	-3.106
	HG	3.361	-5.377	-2.942
	CD1	2.093	-6.866	-2.293
	CD2	2.245	-5.844	-4.610
	HD1	2.633	-7.714	-2.716
	HD1	2.406	-6.717	-1.259
	HD1	1.022	-7.066	-2.324
	HD2	2.856	-6.696	-4.909
	HD2	1.199	-6.049	-4.839
	HD2	2.569	-4.956	-5.153
D-PHE	N	4.078	-3.936	-0.266
	HN	3.746	-4.666	0.332
	CA	5.468	-3.561	-0.063
	HA	5.945	-3.711	-0.929
	CB	6.003	-4.429	1.077
	C*	5.586	-2.088	0.333
	O	4.809	-1.597	1.150
	HB	5.867	-5.479	0.817
	HB	5.408	-4.243	1.972
	CG	7.478	-4.186	1.404
	CD1	8.441	-4.923	0.788
	CD2	7.826	-3.234	2.311
	HD1	8.162	-5.686	0.061
	CE1	9.810	-4.697	1.091
	CE2	9.195	-3.009	2.614
	HD2	7.054	-2.644	2.805
	HE1	10.582	-5.288	0.598
	CZ	10.158	-3.745	1.998
	HE2	9.473	-2.246	3.341
	HZ	11.209	-3.572	2.231
L-PRO	NP	6.591	-1.407	-0.281
	CD	7.530	-1.956	-1.254
	CA	6.821	0.0	0.0
	HA	6.733	0.177	0.980
	CB	8.231	0.274	-0.498
	C*	5.766	0.874	-0.681
	O	5.589	2.036	-0.317
	HB	8.286	1.239	-1.002
	HB	8.938	0.307	0.331
	CG	8.564	-0.860	-1.453
	HG	8.551	-0.506	-2.484
	HG	9.567	-1.240	-1.259
	HD	7.031	-2.205	-2.190
	HD	7.992	-2.873	-0.885
L-VAL	N	5.092	0.282	-1.656
	HN	5.242	-0.663	-1.945
	CA	4.059	0.993	-2.390
	HA	4.292	1.965	-2.374
	CB	4.044	0.532	-3.849
	C*	2.714	0.798	-1.688
	O	2.067	-0.235	-1.854
	HB	3.862	-0.451	-3.860
	CG2	5.403	0.766	-4.512
	CG1	2.926	1.225	-4.631
	HG1	3.038	1.010	-5.694
	HG1	1.959	0.858	-4.286
	HG1	2.983	2.302	-4.470
	HG2	5.322	0.576	-5.582
	HG2	5.714	1.798	-4.349
	HG2	6.140	0.092	-4.077
L-ORN	N	2.333	1.806	-0.918
	HN	2.865	2.643	-0.788
	CA	1.076	1.759	-0.189
	HA	0.586	0.942	-0.495
	CB	1.404	1.700	1.304
	C*	0.237	3.000	-0.498
	O	0.701	4.126	-0.328
	HB	1.989	2.575	1.587
	HB	0.461	1.733	1.884
	CG	2.181	0.427	1.645
	HG	1.683	-0.437	1.205
	HG	3.178	0.477	1.207
	CD	2.292	0.242	3.160
	HD	2.740	1.129	3.609
	HD	1.298	0.132	3.593
	NE	3.112	-0.949	3.478
	HE	2.990	-1.421	4.351
	HE	3.787	-1.281	2.819

<sup>a</sup> The z axis is coincident with the C<sub>2</sub> symmetry axis. <sup>b</sup> Because of possible errors in the bond lengths, bond angles, and potential functions used in the computations, the fourth (and probably third) significant figures are probably not accurate.

tion that agreement within 20° in all dihedral angles was not satisfied). During the process of energy minimization which was accompanied by an average change of backbone dihedral angles of  $\pm 28^\circ$  (for these four starting conformations), these starting conformations all led to an identical minimum-energy conformation. The fact that we obtain one low-energy minimum by starting from all previously published conformations, and that it is the same as the global minimum-energy conformation obtained in this study, appears to support our previous contention that there is only one conformational subspace with distinctly low conformational energy.

The cartesian coordinates of structure M1 are given in Table VIII, for possible comparison with a future X-ray structure determination of Gramicidin S.

### III. Discussion

The entire process of computation described in sections I-A and I-I was organized in such a way as to obtain the global minimum-energy conformation with the least amount of computation. In the initial step, conformations from as much of conformational space as possible were sampled with emphasis on the chemically likely subspace. At later stages, the number of conformations was reduced in several steps by discarding conformations which were judged not likely to lead to the global minimum-energy conformation. However, there are a few assumptions contained in the above computational procedures which may affect the power of the method to attain the final goal. Even though Gramicidin S is a very constrained system, and the number of variables is reduced very much by the symmetry consideration, still the entire conformational space is too large to permit a thorough search. Thus, we focused on the region of conformational space in which the global minimum is likely to exist. The judgment of the likelihood involves an assumption. A second assumption concerns the decisions made in the process of reducing the number of conformations. The most crucial of these was the decision to discard conformations using only the criterion of high energy; if it was high after a few cycles of minimization, the conformation was judged not likely to reach the global minimum. Because of these assumptions we cannot be completely certain that the lowest energy conformation obtained is the real global minimum conformation. However, the lowest energy conformation obtained in this study in fact is judged to be the global minimum because of the following three reasons: (a) the plausibility of the methods employed to generate initial conformations, and the subsequent methods of reducing their number; (b) the way in which low-energy conformations are related to each other as was discussed in section II-A; and (c) the consistency of the computed low-energy result with experimental data as was discussed in section II-B.

The development of a mathematical method for obtaining closed rings, and the maintenance of this condition throughout the energy minimization, is a significant advance in the methodology for studying cyclic peptides. By employing such a technique to eliminate the element of chance in obtaining closed rings, the conformational space of Gr-S has been explored thoroughly, and the global minimum has been located. As a consequence of this thorough search, the conformation of Gr-S predicted previously<sup>26,39-41,43</sup> by less rigorous methods is now established on a firm basis.

### Appendix I

**Derivation of Equations for  $\omega_3$  and  $\omega_9$ .** The condition that **U** and **p** must satisfy for the case of C<sub>2</sub> symmetry is given<sup>3</sup> by eq 7 of the text, viz.,

$$(\mathbf{I} + \mathbf{U})\mathbf{p} = 0 \quad (\text{A-1})$$

Substituting eq 8 and 9 into this gives, upon rearrangement,

$$\mathbf{a} + \mathbf{AXb} + \mathbf{AXB\mathbf{Y}a} + \mathbf{AXBYAXb} = 0 \quad (\text{A-2})$$

which can be transformed to

$$\mathbf{Y}(\mathbf{a} + \mathbf{AXb}) = -\mathbf{B}^{-1}\mathbf{X}^{-1}\mathbf{c} - \mathbf{d} \quad (\text{A-3})$$

with

$$\mathbf{c} = \mathbf{A}^{-1}\mathbf{a} \quad (\text{A-4})$$

and

$$\mathbf{d} = \mathbf{B}^{-1}\mathbf{b} \quad (\text{A-5})$$

From the  $x$  component of eq A-3, we have

$$\alpha \cos \omega_3 + \beta \sin \omega_3 + \gamma = 0 \quad (\text{A-6})$$

where

$$\alpha = b_2a_{12} + b_3a_{13} + c_2b_{21} + c_3b_{31} \quad (\text{A-7})$$

$$\beta = b_2a_{13} - b_3a_{12} + c_3b_{21} - c_2b_{31} \quad (\text{A-8})$$

$$\gamma = a_1 + b_1a_{11} + c_1b_{11} + d_1 \quad (\text{A-9})$$

where  $a_i$ ,  $b_i$ ,  $c_i$ , and  $d_i$  are the  $i$ th components of vectors  $\mathbf{a}$ ,  $\mathbf{b}$ ,  $\mathbf{c}$ , and  $\mathbf{d}$ , respectively, and  $a_{ij}$  and  $b_{ij}$  are the  $i,j$  elements of the matrices  $\mathbf{A}$  and  $\mathbf{B}$ . Equation A-6 contains the unknown quantity  $\omega_3$ . The necessary and sufficient condition for the existence of solution(s) of eq A-6 is given by

$$\alpha^2 + \beta^2 - \gamma^2 \geq 0 \quad (\text{A-10})$$

When this is satisfied, eq A-6 has the solution

$$\begin{aligned} \cos \omega_3 &= \frac{-\alpha\gamma \pm \beta(\alpha^2 + \beta^2 - \gamma^2)^{1/2}}{\alpha^2 + \beta^2} \\ \sin \omega_3 &= \frac{-\beta\gamma \mp \alpha(\alpha^2 + \beta^2 - \gamma^2)^{1/2}}{\alpha^2 + \beta^2} \end{aligned} \quad (\text{A-11})$$

from which  $\omega_3$  can be obtained. Once  $\omega_3$  is found,  $\omega_9$  can be obtained using the  $y$  and  $z$  components of eq A-3. We write eq A-3 as

$$\mathbf{Y}\mathbf{e} = \mathbf{f} \quad (\text{A-12})$$

where

$$\mathbf{e} = \mathbf{a} + \mathbf{AXb} \quad (\text{A-13})$$

and

$$\mathbf{f} = -\mathbf{B}^{-1}\mathbf{X}^{-1}\mathbf{c} - \mathbf{d} \quad (\text{A-14})$$

Equating the  $y$  components of eq A-12 gives

$$e_2 \cos \omega_9 - e_3 \sin \omega_9 = f_2 \quad (\text{A-15})$$

Equating the  $z$  components gives

$$e_2 \sin \omega_9 + e_3 \cos \omega_9 = f_3 \quad (\text{A-16})$$

Equations A-15 and A-16 yield one solution,  $\omega_9$ , for each value of  $\omega_3$ . The independent variables,  $\omega_1$ ,  $\omega_2$ ,  $\omega_4$ , ...,  $\omega_8$ , appear in the quantities  $\mathbf{A}$ ,  $\mathbf{B}$ ,  $\mathbf{a}$ , and  $\mathbf{b}$  of eq 10–13 of the text.

## References and Notes

- (1) This work was supported by research grants from the National Institute of Arthritis and Metabolic Diseases of the National Institutes of Health, U.S. Public Health Service (AM-13743), from the National Science Foundation (BMS71-00872-A04), and from Walter and George Todd.

- (2) NIH Predoctoral Trainee.
- (3) N. Gö and H. A. Scheraga, *Macromolecules*, **6**, 273 (1973).
- (4) F. A. Momany, R. F. McGuire, A. W. Burgess, and H. A. Scheraga, *J. Phys. Chem.*, in press. A preliminary version of these data has been published elsewhere.<sup>5</sup>
- (5) P. N. Lewis, F. A. Momany, and H. A. Scheraga, *Isr. J. Chem.*, **11**, 121 (1973).
- (6) G. M. J. Schmidt, D. C. Hodgkin, and B. M. Oughton, *Biochem. J.*, **65**, 744 (1957).
- (7) A. Stern, W. A. Gibbons, and L. C. Craig, *Proc. Natl. Acad. Sci. U.S.A.*, **61**, 734 (1968).
- (8) A. M. Liquori and F. Conti, *Nature (London)*, **217**, 635 (1968).
- (9) W. A. Gibbons, J. A. Sogn, A. Stern, L. C. Craig, and L. F. Johnson, *Nature (London)*, **227**, 840 (1970).
- (10) F. A. Bovey, *Pept.: Chem. Biochem., Proc. Am. Pept. Symp.*, **3rd**, 3 (1972).
- (11) IUPAC-IUB Commission on Biochemical Nomenclature, *Biochemistry*, **9**, 3471 (1970).
- (12) F. A. Momany, L. M. Carruthers, R. F. McGuire, and H. A. Scheraga, *J. Phys. Chem.*, **78**, 1595 (1974).
- (13) R. F. McGuire, F. A. Momany, and H. A. Scheraga, *J. Phys. Chem.*, **76**, 375 (1972).
- (14) P. K. Warne and H. A. Scheraga, *J. Comput. Phys.*, **12**, 49 (1973).
- (15) R. A. Scott, G. Vanderkooi, R. W. Tuttle, P. M. Shames, and H. A. Scheraga, *Proc. Natl. Acad. Sci. U.S.A.*, **58**, 2204 (1967).
- (16) N. Gö and H. A. Scheraga, *Macromolecules*, **6**, 525 (1973).
- (17) R. Fletcher and M. J. D. Powell, *Comput. J.*, **6**, 163 (1963).
- (18) W. C. Davidson, "A.E.C. Research and Development Report", ANL-5990, 1959.
- (19) For a review of experimental data concerning Gr-S and its corresponding structural implications, see: (a) D. W. Urry and M. Ohnishi, "Spectroscopic Approaches to Biomolecular Conformation", D. W. Urry, Ed., American Medical Association, Chicago, Ill., 1970, p. 263; (b) H. R. Wyssbrod and W. A. Gibbons, "Survey of Progress in Chemistry", Vol. 6, A. F. Scott, Ed., Academic Press, New York, N.Y., 1973.
- (20) W. A. Gibbons, G. Nemethy, A. Stern, and L. C. Craig, *Proc. Natl. Acad. Sci. U.S.A.*, **67**, 239 (1970).
- (21) D. N. Silverman and H. A. Scheraga, *Biochemistry*, **10**, 1340 (1971).
- (22) D. Kotelchuck, H. A. Scheraga, and R. Walter, *Proc. Natl. Acad. Sci. U.S.A.*, **69**, 3629 (1972).
- (23) V. F. Bystrov, S. L. Portnova, V. I. Tsetlin, V. T. Ivanov, and Yu. A. Ovchinnikov, *Tetrahedron*, **25**, 493 (1969).
- (24) G. N. Ramachandran, R. Chandrasekaran, and K. D. Kopple, *Biopolymers*, **10**, 2113 (1971).
- (25) V. F. Bystrov, V. T. Ivanov, S. L. Portnova, T. A. Balashova, and Yu. A. Ovchinnikov, *Tetrahedron*, **29**, 873 (1973).
- (26) Yu. A. Ovchinnikov, V. T. Ivanov, V. F. Bystrov, A. I. Miroshnikov, E. N. Shepel, N. D. Abdullaev, E. S. Efremov, and L. B. Senyavina, *Biochem. Biophys. Res. Commun.*, **39**, 217 (1970).
- (27) N. Gö and H. A. Scheraga, *Macromolecules*, **3**, 188 (1970).
- (28) It has recently been shown<sup>29</sup> that the minimum in  $\psi$  (at  $\omega = 180^\circ$ ) occurs at  $80^\circ$  for *N*-acetyl-*N'*-methylprolineamide. However, the variation in the energy in the region from  $\psi = 80$  to  $160^\circ$  is  $<1$  kcal/mol, with very shallow minima at  $80$ – $85^\circ$  and at  $150^\circ$ . Thus, the value of  $120^\circ$  was selected as a representative one in this whole region. In strategies B and C, this region was sampled more thoroughly. Another minimum (slightly higher in energy) exists at ca.  $-55^\circ$ .<sup>29</sup>
- (29) A. W. Burgess, F. A. Momany, and H. A. Scheraga, *Proc. Natl. Acad. Sci. U.S.A.*, **70**, 1456 (1973); **71**, 4640 (1974).
- (30) S. G. Laland, O. Froyshov, C. Gilhuus-Moe, and T. L. Zimmer, *Nature (London)*, *New Biol.*, **239**, 43 (1972).
- (31) A. W. Burgess, P. K. Ponnuswamy, and H. A. Scheraga, *Isr. J. Chem.*, **12**, 239 (1974).
- (32) C. M. Venkatachalam, *Biopolymers*, **6**, 1425 (1968).
- (33) S. S. Zimmerman and H. A. Scheraga, manuscript in preparation.
- (34) S. L. Laiken, M. P. Printz, and L. C. Craig, *Biochemistry*, **8**, 519 (1969).
- (35) M. Ohnishi and D. W. Urry, *Biochem. Biophys. Res. Commun.*, **36**, 194 (1969).
- (36) W. A. Gibbons, H. Alms, R. S. Bockman, and H. R. Wyssbrod, *Biochemistry*, **11**, 1721 (1972).
- (37) K. D. Kopple, A. Gö, T. J. Schamper, and C. S. Wilcox, *J. Am. Chem. Soc.*, **95**, 6090 (1973).
- (38) H. A. Scheraga, *Pure Appl. Chem.*, **36**, 1 (1973).
- (39) D. C. Hodgkin and B. M. Oughton, *Biochem. J.*, **65**, 752 (1957).
- (40) R. Schwyzer, *Chimia*, **12**, 53 (1958).
- (41) R. Schwyzer, *Rec. Chem. Prog.*, **20**, 147 (1959).
- (42) F. A. Momany, G. Vanderkooi, R. W. Tuttle, and H. A. Scheraga, *Biochemistry*, **8**, 744 (1969).
- (43) P. De Santis and A. M. Liquori, *Biopolymers*, **10**, 699 (1971).
- (44) R. Chandrasekaran, A. V. Lakshminarayanan, U. V. Pandya, and G. N. Ramachandran, *Biochim. Biophys. Acta*, **303**, 14 (1973).
- (45) A. M. Liquori, P. De Santis, A. L. Kovacs, and L. Mazzarella, *Nature (London)*, **211**, 1039 (1966).
- (46) G. Vanderkooi, S. J. Leach, G. Nemethy, R. A. Scott, and H. A. Scheraga, *Biochemistry*, **5**, 2991 (1966).